Recent progress on phase-mask coronagraphy based on photonic-crystal technology

Naoshi Murakami*[a,b], Jun Nishikawa[c,d], Motohide Tamura[e,c], Eugene Serabyn[b], Wesley A. Traub[b], Kurt M. Liewer[b], Dwight C. Moody[b], John T. Trauger[b], Olivier Guyon[f,g], Frantz Martinache[h], Nemanja Jovanovic[f], Garima Singh[f], Fumika Oshiyama[i], Hayato Shoji[i], Moritsugu Sakamoto[i], Shoki Hamaguchi[i], Kazuhiko Oka[a], Naoshi Baba[a]

[a]Faculty of Engineering, Hokkaido University, Kita-13, Nishi-8, Kita-ku, Sapporo, Hokkaido, 060-8628, Japan; [b]Jet Propulsion Laboratory, California Institute of Technology, 4800 Oak Grove Drive, Pasadena, CA, 91109, USA; [c]Extrasolar Planet Project Office, National Astronomical Observatory of Japan, 2-21-1, Osawa, Mitaka, Tokyo, 181-8588 Japan; [d]The School of Physical Sciences, The Graduate University for Advanced Studies, 2-21-1, Osawa, Mitaka, Tokyo, 181-8588 Japan; [e]Graduate School of Science, The University of Tokyo, 7-3-1 Hongo, Bunkyo-ku, Tokyo, 113-0033, Japan; [f]National Astronomical Observatory of Japan, Subaru Telescope, 650 N. A'ohoku Place, Hilo, HI, 96720, USA; [g]University of Arizona, 933 N Cherry Ave., Tucson, AZ, 85721, USA; [h]Laboratoire Lagrange, CNRS UMR 7293, Observatoire de la Cote d'Azur, Boulevard de l'Observatoire, Nice, 06304, France; [i]Graduate School of Engineering, Hokkaido University, Kita-13, Nishi-8, Kita-ku, Sapporo, Hokkaido, 060-8628, Japan

ABSTRACT

We have been developing focal-plane phase-mask coronagraphs ultimately aiming at direct detection and characterization of Earth-like extrasolar planets by future space coronagraph missions. By utilizing photonic-crystal technology, we manufactured various coronagraphic phase masks such as eight-octant phase masks (8OPMs), 2nd-order vector vortex masks, and a 4th-order discrete (32-sector) vector vortex mask. Our laboratory experiments show that the 4th-order vortex mask reaches to higher contrast than the 2nd-order one at inner region on a focal plane. These results demonstrate that the higher-order vortex mask is tolerant of low-order phase aberrations such as tip-tilt errors. We also carried out laboratory demonstration of the 2nd-order vector vortex masks in the High-Contrast Imaging Testbed (HCIT) at the Jet Propulsion Laboratory (JPL), and obtained 10^{-8}-level contrast owing to an adaptive optics system for creating dark holes. In addition, we manufactured a polarization-filtered 8OPM, which theoretically realizes achromatic performance. We tested the manufactured polarization-filtered 8OPM in the Infrared Coronagraphic Testbed (IRCT) at the JPL. Polychromatic light sources are used for evaluating the achromatic performance. The results suggest that 10^{-5}-level peak-to-peak contrasts would be obtained over a wavelength range of 800-900 nm. For installing the focal-plane phase-mask coronagraph into a conventional centrally-obscured telescope with a secondary mirror, pupil-remapping plates have been manufactured for removing the central obscuration to enhance the coronagraphic performance. A result of preliminary laboratory demonstration of the pupil-remapping plates is also reported. In this paper, we present our recent activities of the photonic-crystal phase coronagraphic masks and related techniques for the high-contrast imaging.

Keywords: high-contrast imaging, phase-mask coronagraph, extrasolar planets, photonic crystal

1. INTRODUCTION

High contrast imager is a key instrument for directly imaging extrasolar planets. Recently, several giant planets have been imaged owing to progress of observational instruments[1-3]. Direct imaging of much smaller Earth-like planets is extremely challenging due to overwhelming intensity ratio (contrast) such as 10^{-10} between a planet and its parent star. For direct imaging of the Earth-like planets, it would be necessary to develop advanced coronagraphs that theoretically realize strong suppression of starlight to a level of 10^{-10}.

*nmurakami@eng.hokudai.ac.jp; phone 81 11 706-6720; fax 81 11 706-7811

Space Telescopes and Instrumentation 2014: Optical, Infrared, and Millimeter Wave, edited by Jacobus M. Oschmann, Jr., Mark Clampin, Giovanni G. Fazio, Howard A. MacEwen, Proc. of SPIE Vol. 9143, 914334 · © 2014 SPIE
CCC code: 0277-786X/14/$18 · doi: 10.1117/12.2054790

A focal-plane phase-mask coronagraph is one of promising methods. This method utilizes a phase mask on a telescope focal plane where an astronomical target is imaged. Many kinds of coronagraphic masks have been proposed to date, for example, a four-quadrant, an eight-octant, or other segmented phase masks[4-6]. These masks divide a stellar image into 4*N* sectors (*N* is an integer), and provides π-phase difference between wavefronts passing through adjacent sectors. Then, starlight is destructively interfered inside the reimaged pupil area. The starlight is totally diffracted outside the pupil, and blocked by a diaphragm called Lyot stop. These segmented π-phase masks are regarded as families of optical vortex masks[7], since the segmented phase masks can mathematically be expressed, via complex Fourier series expansion, as weighted sum of optical vortex masks with various topological charges[8].

For realizing achromatic focal-plane phase masks, space-variant half-wave plates (HWPs) have been proposed such as vector vortex masks[9]. These masks manipulate states of polarization to modulate Pancharatnam-Berry's phase[10,11]. The coronagraphic performance can be achromatized by placing the mask between crossed polarization filters. As the polarization filters, crossed linear polarizers would be used for π-phase masks, while crossed circular polarizers would be used for the vector vortex ones.

Photonic crystals are very attractive devices for realizing the coronagraphic phase masks, owing to the extremely small manufacturing defects. Various photonic-crystal phase masks have been manufactured to date, such as the eight-octant phase mask (8OPM)[12,13], continuous vector vortex mask with a topological charge of 2 (so-called 2nd-order mask)[14], 4th-order discrete (32-sector) vector vortex mask, and so on.

The phase-mask coronagraph theoretically realizes perfect rejection of starlight when assuming a telescope pupil without central obscuration due to a secondary mirror. However, the achievable contrast would be severely degraded when the coronagraph is installed into a conventional centrally-obscured telescope. For improving the performance of the phase-mask coronagraph, pupil-remapping plates have been designed to convert the centrally-obscured telescope pupil into a clear circular one[15].

In this paper, we show our recent activities of the photonic-crystal coronagraphic phase masks and related techniques for the high-contrast imaging. In section 2, we outline the photonic-crystal technology and its application to the coronagraphic phase masks. In section 3, we show our laboratory demonstration of the photonic-crystal vector vortex masks and 8OPM in the High-Contrast Imaging Testbed (HCIT) and the Infrared Coronagraphic Testbed (IRCT) at the Jet Propulsion Laboratory (JPL). We also report our preliminary laboratory demonstration of the manufactured pupil remapping plates in section 4. Finally, we summarize our conclusion in section 5.

2. PHOTONIC-CRYSTAL TECHNOLOGY FOR CORONAGRAPHIC PHASE MASKS

Photonic crystal is an artificial periodic nanostructure of high and low refractive indices. Recently, various coronagraphic phase masks have been manufactured, such as an 8OPM[12,13], a 2nd-order continuous vector vortex mask[14], and a 4th-order discrete (32-sector) vector vortex mask. Details of the manufacturing process, schematic cross sectional view, and a scanning electron microscope (SEM) image of the photonic-crystal coronagraphic mask can be seen in the previous publication[12]. The photonic-crystal phase masks are manufactured based on auto-cloning technique[16,17]. First, periodic corrugated pattern is formed, via electron-beam lithography, on a dielectric substrate (e.g., synthetic fused silica). Then, two dielectric materials (e.g., Nb_2O_5 and SiO_2 in our case) are deposited alternatively on the substrate by RF sputtering, preserving the corrugated pattern. The manufactured mask exhibits birefringent characteristics with fast (or slow) axis along orientation angles of the corrugated pattern on the substrate. Thus, a space-variant HWP for the coronagraphic mask can be realized by properly designing the corrugated pattern and the multilayer structure.

Figure 1 shows schematic designs of the manufactured masks. Arrows indicate fast (or slow) axes of the space-variant HWP. These masks provide incoming light with space-variant Pancharatnam-Berry's phase depending on the orientation angles of the fast axes. For example, the 8OPM is composed of eight-octant HWPs with fast axes of ±45°, as shown in figure 1, to provide π-phase difference between the adjacent octant sectors.

As shown in figure 1, the coronagraphic masks have phase singularity at the center and along phase transition lines. The photonic-crystal technology makes it possible to realize the coronagraphic masks with extremely small manufacturing defects of less than 1-μm scale, as can be seen in the SEM image of the manufactured mask[12].

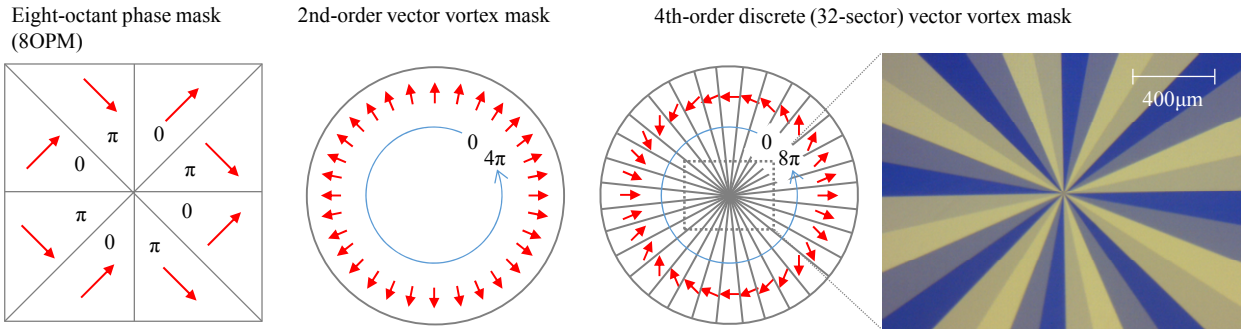

Figure 1. Schematic designs of the manufactured photonic-crystal eight-octant phase mask, 2nd-order continuous vector vortex mask, and 4th-order discrete (32-sector) vector vortex mask. These masks are composed of space-variant half-wave plates (HWPs). Arrows show fast (or slow) axes of the HWP. A microscope image of the discrete vortex mask, placed between two polarizers, is also shown.

3. LABORATORY DEMONSTRATIONS

3.1 Comparison of 2nd- and 4th-order vector vortex masks

The 4th-order 32-sector vector vortex mask is mathematically expressed as weighted sum of optical vortices with various topological charges by utilizing complex Fourier series expansion[8]. A dominant term is an optical vortex with the topological charge of 4 (the designed charge l_{des}). In addition to the dominant term, the other terms with charges $l_{des}\pm N$ are included in the mask function, where N is the number of sectors (N=32 in this case). Thus, the lowest order is 4, and the manufactured discrete vortex mask would exhibit coronagraphic performance similar to a 4th-order vortex mask. Figure 2 shows results of laboratory demonstration of the 2nd-order continuous and the 4th-order discrete vector vortex masks. A monochromatic laser light source with a wavelength of 604 nm is used as a model star. Images on a final focal plane are shown together with the contrast curves. Here, rms intensity variations are calculated as a metric of the contrast. We can see that the contrast obtained by the 4th-order mask is better than that obtained by the 2nd-order mask especially at inner region within ~5λ/D. The results demonstrate that the higher-order mask is tolerant of low-order phase aberrations, which degrade the contrast at the inner region on the focal plane.

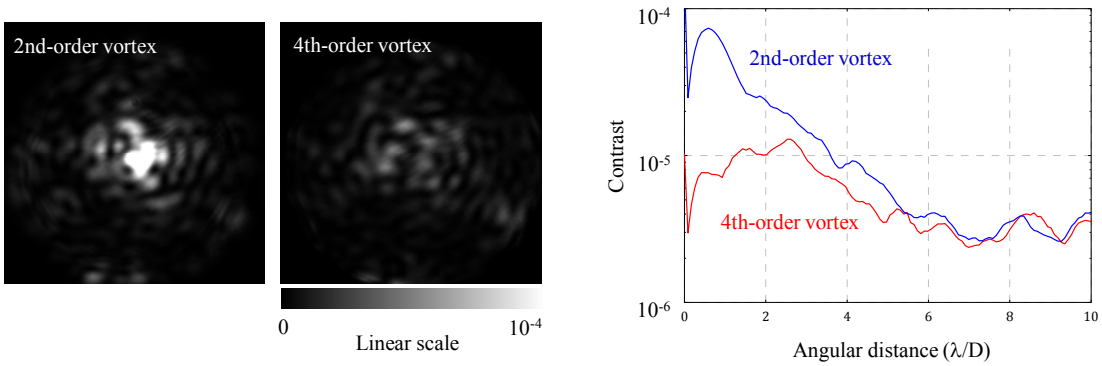

Figure 2. Laboratory coronagraphic demonstration using 2nd-order continuous and 4th-order discrete vector vortex masks.

3.2 Laboratory demonstration of 2nd-order vector vortex masks

We carried out laboratory demonstration of the photonic-crystal vector vortex masks at the Jet Propulsion Laboratory (JPL) using a coronagraphic testbed called High-Contrast Imaging Testbed (HCIT). The HCIT is a state-of-the-art coronagraphic testbed located in very stable environment of a vacuum chamber. Achievable contrasts of the coronagraphs would be limited by residual speckles due to phase aberrations of optical components. The HCIT mounts an adaptive optics system for creating dark hole against the residual speckles by the specially designed algorithm called

electric field conjugation (EFC)[18,19]. With the HCIT, direct imaging at the contrast needed for detection of Earth-like planets has successfully been demonstrated[20]. Laboratory demonstrations of various coronagraphs at the HCIT are summarized in Ref. [21], and the details are described in references therein. We carried out laboratory demonstration of the 2nd-order continuous vector vortex masks shown in figure 1 with different diameters (5 mm and 10 mm, respectively). Figure 3 shows results of the demonstration at the HCIT acquired by using a monochromatic light source with a wavelength of 785 nm. Contrasts of about $1.5(\pm0.3)\times10^{-8}$ and $3.4(\pm0.7)\times10^{-8}$ (over dark-hole regions with a range of 3-12 λ/D) were obtained for the small and large masks, respectively. As observed in the result of the small mask, the contrasts were limited by diffraction-like residual light over the dark-hole region. We assume that the residual light could be due to ghost light created by internal reflections of the masks. The manufactured masks are anti-reflective (AR) coated with reflectance of less than 1%. We expect that appropriately designed masks with better AR coatings could reach to higher contrast.

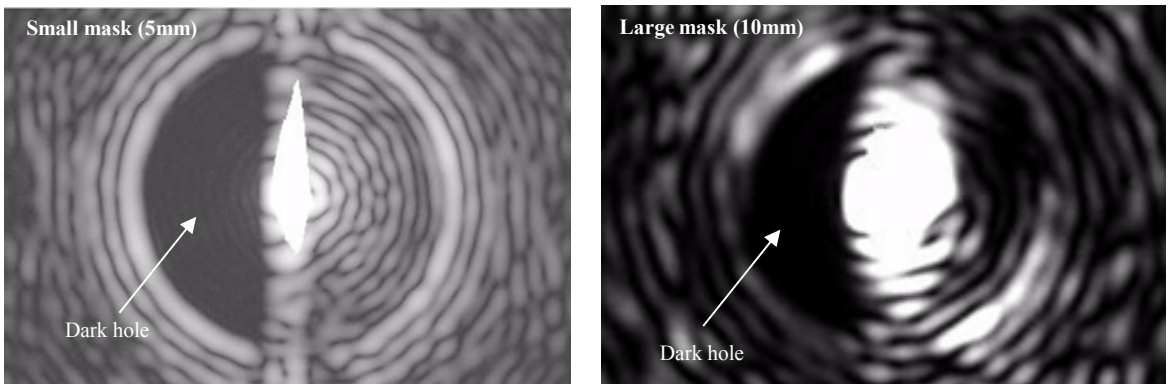

Figure 3. Results of laboratory coronagraphic demonstration at the HCIT/JPL using 2nd-order vector vortex masks with effective diameters of (*left*) 5 mm and (*right*) 10 mm, respectively.

3.3 A polarization-filtered 8-octant phase mask (8OPM)

As mentioned above, polarization filtering is one solution for achromatizing the coronagraphic masks. However, one drawback of the polarization filtering is additional phase aberration due to the polarizers. For mitigating this drawback, we place the polarizers on a focal plane, instead of placing them near a pupil plane. A light beam would be much smaller on a focal plane than that on a pupil plane, resulting in much smaller phase aberrations.

We built an all-in-one polarization-filtered 8OPM. Figure 4 shows a schematic design and a picture of the polarization-filtered 8OPM. The photonic-crystal 8OPM and crossed polarizers are compactly mounted on a single holder so that all optical components can be placed on a focal plane. As the polarizers, we used commercially available one with a thickness of 0.5 mm. We carried out laboratory demonstration of the polarization-filtered 8OPM also at the JPL using another testbed, called Infrared Coronagraphic Testbed (IRCT). The IRCT is a coronagraphic testbed located in air environment, without an adaptive optics system for the EFC algorithm.

Figure 4 also shows experimental results of the polarization-filtered 8OPM at the IRCT. Various light sources with wavelengths from 635 nm to 880 nm are used as a model star to evaluate achromaticity of the coronagraphic mask. A graph shows peak-to-peak contrasts of the acquired images. Horizontal bars in the graph show bandwidths of the light sources. We also show a coronagraphic image obtained with a light source of a wavelength of 798 nm (a bandwidth of 32 nm) for reference. The image is displayed with a logarithmic scale from 10^{-8} to 10^{-5}. As can be seen, 10^{-5}-level peak-to-peak contrasts are obtained over a wavelength range from 800 nm to 900 nm. The graph also shows that the contrast becomes worse at shorter wavelengths. We expect that the degradation of the contrast at the shorter wavelength range would be due to the polarizers used for the mask, since they do not operate well at this wavelength range. Therefore, achromatic higher contrast would be realized by using better polarizers with higher extinction ratio over broader wavelength range.

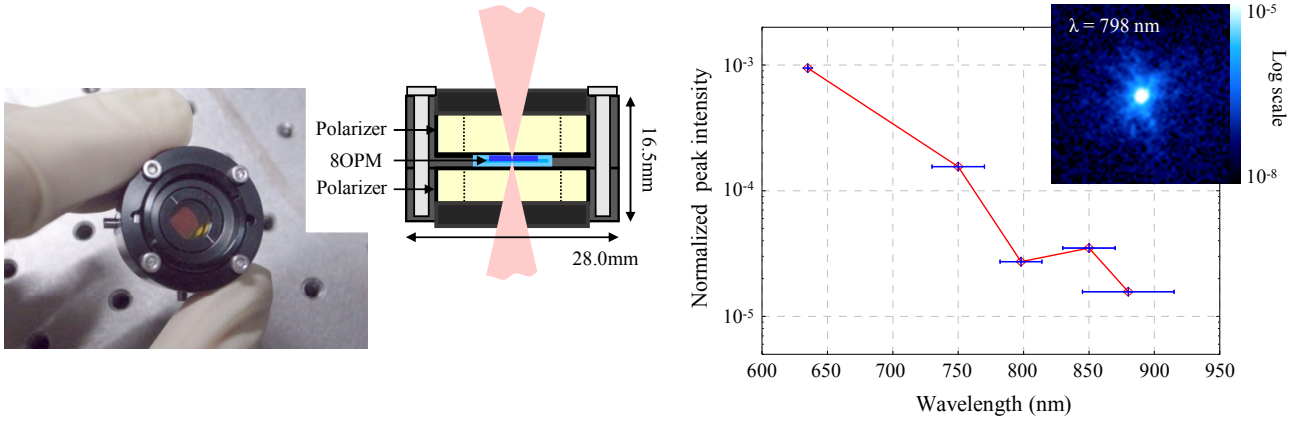

Figure 4. (*Left*) Schematic design and picture of the manufactured polarization-filtered 8-octant phase mask (8OPM). The photonic-crystal 8OPM and two polarizers (only their holders are shown in the design) are compactly mounted on a single holder. (*Right*) Results of laboratory demonstration of the polarization-filtered 8OPM at the IRCT/JPL. A graph shows obtained peak-to-peak contrasts as a function of a wavelength of light sources. Horizontal bars in the graph indicate bandwidths of the light sources. A focal-plane coronagraphic image at a wavelength of 798 nm is also shown.

3.4 Future plan: a three-layer 8OPM for unpolarized light

Another drawback of the polarization-filtered phase masks would be loss of incoming photons due to the polarizers. For overcoming this problem, we designed an achromatic three-layer 8OPM. The three-layer coronagraphic masks have originally been proposed in context of the vector vortex mask[22]. It is expected that the three-layer 8OPM would enable us to realize achromatic and higher contrast without polarization filtering.

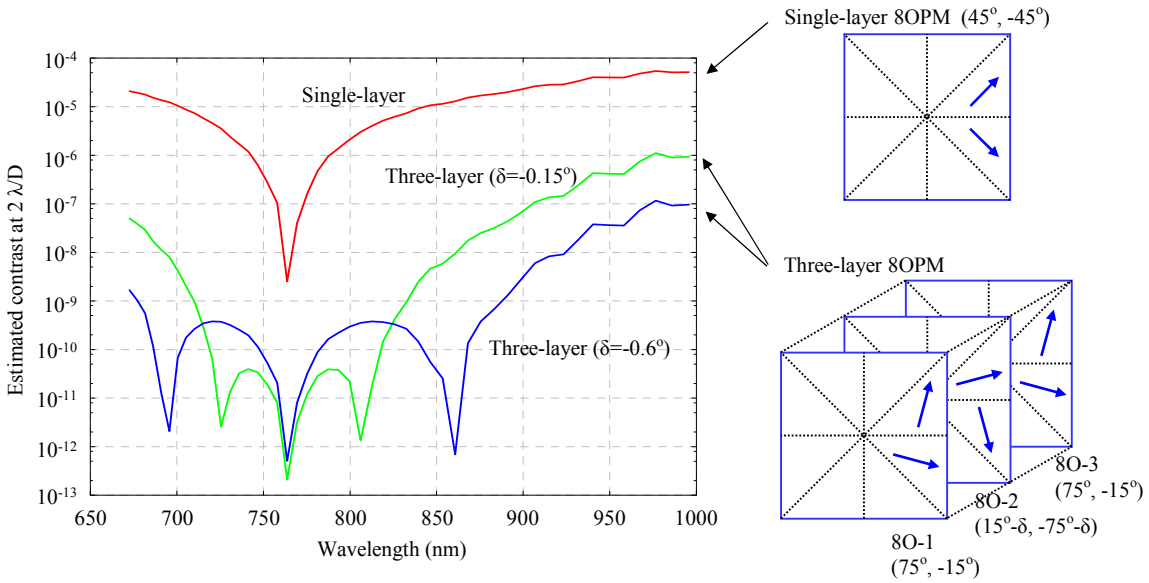

Figure 5. Numerical simulation of estimated contrasts at 2 λ/D assuming single-layer and three-layer photonic-crystal 8OPMs without polarization filtering.

As schematically shown in figure 5, the single-layer photonic-crystal 8OPM is composed of space-variant HWPs with the fast axes of ±45°. On the other hand, the three-layer 8OPM is composed of three eight-octant HWPs with different designs. Fast axes of the eight-octant HWPs are set to 75° and -15° for the first and third masks, while 15°-δ and -75°-δ

for the second one, as illustrated in figure 5. The angle δ is a free parameter for determining an achievable contrast and achromatic performance. A graph in figure 5 shows results of numerical estimation of the achievable contrasts at 2 λ/D as a function of a wavelength for the single- and the three-layer photonic-crystal 8OPMs. For the three-layer 8OPM, the parameter δ is set to -0.15° and -0.6°. The numerical estimations assume that a phase retardation of the photonic-crystal HWP is optimized at a wavelength of roughly 765 nm. The numerical simulation suggests that the three-layer 8OPM can achieve contrast of 10^{-10} over 13% bandwidth (720-820 nm) when δ=-0.15°, while 10^{-9} over 26% bandwidth (680-880 nm) when δ= -0.6°. Manufacturing of the high-performance three-layer photonic-crystal 8OPM is our important future-planned work.

4. DEVELOPMENT OF CENTRAL-OBSCURATION REMOVAL PLATES

On-sky observations using the focal-plane phase-mask coronagraphs mounted onto ground-based large telescopes would be an important step for proceeding to future space coronagraph missions. The Subaru Coronagraphic Extreme Adaptive Optics (SCExAO) is one attractive possibility for on-sky observations with the 8OPM coronagraph[23,24]. However, the existing telescopes have secondary mirrors which obscure a central part of the telescope pupil, resulting in degradation of the coronagraphic performance. Several approaches have been proposed for mitigating the effect of the central obscuration on the coronagraphic performance[25-27].

Pupil-remapping plates were designed for transforming the centrally-obscured telescope pupil into a clear circular one[15]. Figure 6 shows a schematic design of the pupil-remapping plates, which is called central-obscuration removal plates (CRPs). The first plate is plano-convex, while the second one is plano-concave. Optical surface shapes of these plates are designed in order to remap an incoming centrally-obscured beam (with outer and inner diameters of *D* and *aD*, respectively) to a clear circular one (with a diameter of *D*). We note that, in the schematic design, a scale along *z*-axis is exaggerated to clearly show the convex and concave surfaces of these plates.

The designed CRPs have been manufactured for H-band observations. Low-dispersion magnesium fluoride (MgF_2) was selected as a material of these plates. A picture of the manufactured CRPs is shown in figure 6. The CRPs are mounted on 5-axis lens holders (lateral positions *x, y*, tip θ_x, tilt θ_y, and rotation) for fine optical alignment. We carried out preliminary laboratory tests using a monochromatic He-Ne laser light source (a wavelength of 604 nm). As shown in figure 6, we demonstrated successfully a removal of the central obscuration of a model telescope pupil.

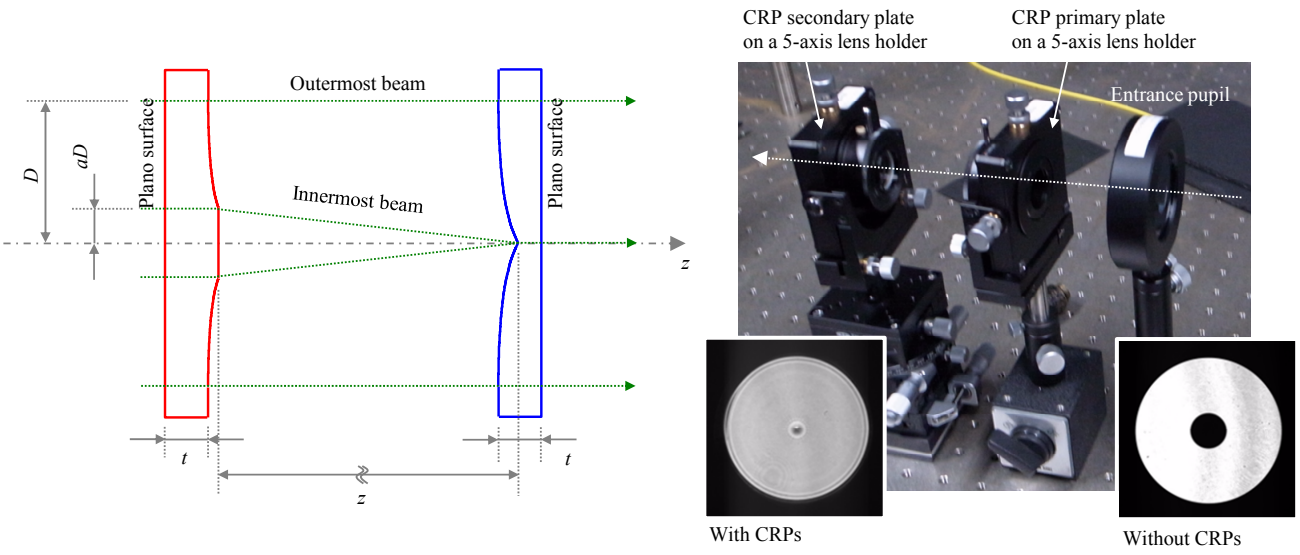

Figure 6. (*Left*) Schematic design and (*right*) picture of the manufactured pupil-remapping plates, which is called central-obscuration removal plates (CRPs). The CRPs are mounted on 5-axis lens holders (*x* and *y* lateral shifts, tip, tilt, and rotation) for fine optical alignment. Experimentally acquired images of a centrally-obscured pupil without and with the CRPs are also shown.

5. CONCLUSION

We have been developing the focal-plane coronagraphic phase masks based on the photonic-crystal technology. The photonic-crystal coronagraphic masks are advantageous because of their extremely small manufacturing defects. Comparison of the 2nd-order (continuous) and the 4th-order (discrete) vortex masks demonstrates that the higher-order vortex mask is tolerant of the low-order phase aberration, resulting in higher contrast especially at the inner region on the final focal plane. Next, we carried out laboratory demonstrations of the 2nd-order vector vortex masks at the HCIT/JPL, combined with the adaptive optics system using the EFC algorithm. We obtained 10^{-8}-level contrasts using a monochromatic light source. We also built the all-in-one polarization-filtered 8OPM, and carried out laboratory demonstrations at the IRCT/JPL. It is expected that the all-in-one polarization-filtered 8OPM reduces phase aberration by placing all optical components on the focal plane where the beam size is much smaller than that on the pupil plane. Although the laboratory demonstration was carried out without the adaptive optics system, 10^{-5}-level peak-to-peak contrasts could be obtained over a wavelength range of 800-900 nm. Finally, development of the high-performance three-layer 8OPM and the CRPs, and other related subsystems such as polarimetric observation mode, would be our important future works for realizing strategic planet-finding missions with high-performance coronagraphic system.

ACKNOWLEDGEMENTS

We acknowledge Takayuki Kawashima of the Photonic Lattice Inc. for providing us with useful information on the photonic crystal technology. We are grateful to Taro Matsuo of Kyoto University for his useful comments on the 8OPM/SCExAO development. This works were carried out at Hokkaido University, the National Astronomical Observatory of Japan (NAOJ), and the Jet Propulsion Laboratory (JPL), California Institute of Technology, under a contract with the National Aeronautics and Space Administration (NASA). This research was partially supported by the NAOJ, the Japan Aerospace Exploration Agency (JAXA), JSPS KAKENHI (Grant Numbers 23740139, 25610038), and MEXT KAKENHI (Grant Number 24103501). NM is supported also by JSPS KAKENHI (Grant Number 26287026). MT is supported by JSPS KAKENHI (Grant Number 22000005).

REFERENCES

[1] Marois, C., Macintosh, B., Barman, T., Zuckerman, B., Song, I., Patience, J., Lafrenière, D. and Doyon, R., "Direct imaging of multiple planets orbiting the star HR 8799," Science 322, 1348-1352 (2008).

[2] Lagrange, A.-M., Bonnefoy, M., Chauvin, G., Apai, D., Ehrenreich, D., Boccaletti, A., Gratadour, D., Rouan, D., Mouillet, D., Lacour, S. and Kasper, M., "A giant planet imaged in the disk of the young star β Pictoris," Science 329, 57-59 (2010).

[3] Kuzuhara, M., Tamura, M., Kudo, T., Janson, M., Kandori, R., Brandt, T. D., Thalmann, C., Spiegel, D., Biller, B., Carson, J., Hori, Y., Suzuki, R., Burrows, A., Henning, T., Turner, E. L., McElwain, M. W., Moro-Martín, A., Suenaga, T., Takahashi, Y. H., Kwon, J., Lucas, P., Abe, L., Brandner, W., Egner, S., Feldt, M., Fujiwara, H., Goto, M., Grady, C. A., Guyon, O., Hashimoto, J., Hayano, Y., Hayashi, M., Hayashi, S. S., Hodapp, K. W., Ishii, M., Iye, M., Knapp, G. R., Matsuo, T., Mayama, S., Miyama, S., Morino, J.-I., Nishikawa, J., Nishimura, T., Kotani, T., Kusakabe, N., Pyo, T.-S., Serabyn, E., Suto, H., Takami, M., Takato, N., Terada, H., Tomono, D., Watanabe, M., Wisniewski, J. P., Yamada, T., Takami, H. and Usuda, T., "Direct imaging of a cold Jovian exoplanet in orbit around the Sun-like star GJ 504," Astrophys. J. 774, 11 (18 pp) (2013).

[4] Rouan, D., Riaud, P., Boccaletti, A., Clénet, Y. and Labeyrie, A., "The four-quadrant phase-mask coronagraph. I. principle," Publ. Astron. Soc. Pacific 112, 1479-1486 (2000).

[5] Murakami, N., Uemura, R., Baba, N., Nishikawa, J., Tamura, M., Hashimoto, N. and Abe, L., "An eight-octant phase-mask coronagraph," Publ. Astron. Soc. Pacific 120, 1112-1118 (2008).

[6] Carlotti, A., Ricort, G. and Aime, C., "Phase mask coronagraphy using a Mach-Zehender interferometer," Astron. Astrophys. 504, 663-671 (2009).

[7] Foo, G., Palacios, D. M. and Swartzlander, Jr., G. A., "Optical vortex coronagraph," Opt. Lett. 30(24), 3308-3310 (2005).
[8] Swartzlander, Jr., G. A., "Broadband nulling of a vortex phase mask," Opt. Lett. 30, 2876-2878 (2005).
[9] Mawet. D., Riaud, P., Absil, O. and Surdej, J., "Annular groove phase mask coronagraph," Astrophys. J. 633, 1191-1200 (2005).
[10] Pancharatnam, S., "Generalized theory of interference, and its applications," Proc. Indian Acad. Sci. 44, 247-262 (1956).
[11] Berry, M., "The adiabatic phase and Pancharatnam's phase for polarized light," J. Mod. Opt. 34, 1401-1407 (1987).
[12] Murakami, N., Nishikawa, J., Yokochi, K., Tamura, M., Baba, N. and Abe, L., "Achromatic eight-octant phase-mask coronagraph using photonic crystal," Astrophys. J. 714, 772-777 (2010).
[13] Murakami, N., Nishikawa, J., Traub, W. A., Mawet, D., Moody, D. C., Kern, B. D., Trauger, J. T., Serabyn, E., Hamaguchi, S., Oshiyama, F., Sakamoto, M., Ise, A., Oka, K., Baba, N., Murakami, H. and Tamura, M., "Coronagraph focal-plane phase-masks based on photonic crystal technology: recent progress and observational strategy," Proc. SPIE 8442, 844205-1-844205-9 (2012).
[14] Murakami, N., Hamaguchi, S., Sakamoto, M., Fukumoto, R., Ise, A., Oka, K., Baba, N. and Tamura, M., "Design and laboratory demonstration of an achromatic vector vortex coronagraph," Opt. Express 21, 7400-7410 (2013).
[15] Oshiyama, F., Murakami, N., Guyon O., Martinache, F., Baba, N., Matuso, T., Nishikawa, J. and Tamura, M., "Central-obscuration removal plates for focal-plane phase-mask coronagraphs with a centrally-obscured telescope," Publ. Astron. Soc. Pacific 126, 270-279 (2014).
[16] Kawakami, S., Kawashima, T. and Sato, T, "Mechanism of shape formation of three-dimensional periodic nanostructures by bias sputtering," Appl. Phys. Lett. 74, 463-465 (1999).
[17] Kawashima, T., Miura, K., Sato, T. and Kawakami, S., "Self-healing effects in the fabrication process of photonic crystals," Appl. Phys. Lett. 77, 2613-2615 (2000).
[18] Bordé, P. J. and Traub, W. A., "High-Contrast Imaging from Space: Speckle Nulling in a Low-Aberration Regime," Astrophys. J. 638, 488-498 (2006).
[19] Give'on, A., Kern, B., Shaklan, S., Moody, D. C., and Pueyo, L., "Broadband wavefront correction algorithm for high-contrast imaging systems," Proc. SPIE 6691, 66910A-1-66910A-11 (2007).
[20] Trauger, J. T. and Traub, W. A. "A laboratory demonstration of the capability to image an Earth-like extrasolar planet," Nature 446, 771-773 (2007).
[21] Lawson, P. R., Belikov, R., Cash, W., Clampin, M., Glassman, T., Guyon, O., Kasdin, N. J., Kern, B. D., Lyon, R., Mawet, D., Moody, D., Samuele, R., Serabyn, E., Sirbu, D., Trauger, J., "Survey of experimental results in high-contrast imaging for future exoplanet missions," Proc. SPIE 8864, 88641F-1-88641F-8 (2013).
[22] Mawet, D., Pueyo, L., Moody, D., Krist, J. and Serabyn, E., "The Vector Vortex Coronagraph: sensitivity to central obscuration, low-order aberrations, chromaticism, and polarization," Proc. SPIE 7739, 773914-1-773914-13 (2010).
[23] Martinache, F. and Guyon, O., "The Subaru coronagraphic extreme AO project," Proc. SPIE 7440, 74400O-1-74400O-9 (2009).
[24] Murakami, N., Guyon, O., Martinache, F., Matsuo, T., Yokochi, K., Nishikawa, J., Tamura, M., Kurokawa, T., Baba, N., Vogt, F., Garrel, V. and Yoshikawa, T., "An eight-octant phase-mask coronagraph for the Subaru coronagraphic extreme AO (SCExAO) system: system design and expected performance," Proc. SPIE 7735, 773533-1-773533-7 (2010).
[25] Murakami, N. and Baba, N., "Pupil-remapping mirrors for a four-quadrant phase mask coronagraph," Publ. Astron. Soc. Pacific 117, 295-299 (2005).
[26] Abe, L., Murakami, N., Nishikawa, J. and Tamura, M., "Removal of central obscuration and spider arm effects with beam-shaping coronagraphy," Astron. Astrophys. 451, 363-373 (2006).
[27] Mawet, D., Pueyo, L., Carlotti, A., Mennesson, B., Serabyn, E. and Wallace, J. K., "Ring-apodized vortex coronagraphs for obscured telescopes. I. transmissive ring apodizers," Astrophys. J. 209, 7 (8pp) (2013).